CHEMISTRY
A EUROPEAN JOURNAL

DOI: 10.1002/chem.200801092

Structure Elucidation and Theoretical Investigation of Key Steps in the Biogenetic Pathway of Schisanartane Nortriterpenoids by Using DFT Methods

Wei-Lie Xiao,[a] Chun Lei,[a] Jie Ren,[a] Tou-Gen Liao,[a] Jian-Xin Pu,[a] Charles U. Pittman, Jr.,[b] Yang Lu,[c] Yong-Tang Zheng,[d] Hua-Jie Zhu,*[a] and Han-Dong Sun*[a]

Abstract: Rubrifloradilactone C (**4**), a novel bioactive nortriterpenoid, along with four other nortriterpenoids (**1**–**3**, **5**) were isolated from *Schisandra rubriflora*. The structure of **4** was determined by extensive NMR spectral analysis, computational evidence by using the GIAO method at the B3LYP/6–311++G(2d,p)//B3LYP/6–31G(d) levels, and X-ray analysis. DFT at the B3LYP/6–311+G(d,p) level was selected to clarify the key mechanistic steps in the formation of **1** and **4** through transition-state (TS) investigations. The effect of enzymes on the TS barriers was considered by using the polarized continuum model. Other possible products based on the new mechanism were predicted.

Keywords: biogenetic pathway · biological activity · density functional calculations · nortriterpenoids · X-ray absorption spectroscopy

Introduction

Triterpenoids are a large and structurally diverse group of natural products derived from squalene or related acyclic 30-carbon precursors, the most ubiquitous, nonsteroidal secondary metabolites in terrestrial and marine flora and fauna. This large group of natural products displays well over 100 different skeletons[1] with different biological properties, such as anti-inflammatory,[2] anticancer,[2] antimicrobial;[2] and many plant defense functions.[3] Although over 20000 members of this group are already known to exist, new triterpenoid structures with novel skeletons and representing unique biosynthetic end products continue to emerge. These complex triterpenoid structures generated great interest and challenges to chemists performing biogenetic studies,[3–5] including the use of quantum mechanics to provide deeper mechanistic insight.[6]

Plants of the genus *Schisandra* in the Schisandraceae family have a long history of use as sedative and tonic agents in Traditional Chinese Medicine. Previous studies showed that this genus is a rich source of dibenzocyclooctadiene lignans, which have been found to possess some beneficial pharmacological effects, including anti-HIV, antitumor, and antihepatitis activities.[7] To find new, natural compounds with interesting biological activities from this genus, more than 50 highly oxygenated nortriterpenoids have been isolated and characterized by our group since 2003.[8] These compounds include schisanartane (e.g. **1**),[8a] schiartane (e.g. **2**),[8a,b] and 18-norschiartane (e.g. **3**)[8a,c] types of nortriterpenoids, some of which showed anti-HIV activity.[8b,g] Recently, we obtained the new compound rubrifloradilactone C (**4**),

[a] Dr. W.-L. Xiao, C. Lei, J. Ren, T.-G. Liao, J.-X. Pu, Prof. H.-J. Zhu, H.-D. Sun
State Key Laboratory of Phytochemistry and Plant Resources in West China
Kunming Institute of Botany, Chinese Academy of Sciences
Heilongtan, Kunming 650204, Yunnan (China)
Fax: (+86) 871-521-6343
E-mail: hjzhu@mail.kib.ac.cn
hdsun@mail.kib.ac.cn

[b] Prof. C. U. Pittman, Jr.
Department of Chemistry, Mississippi State University
Mississippi State, 39762, MS (USA)

[c] Prof. Y. Lu
Institute of Materia Medica
Chinese Academy of Medical Sciences
Beijing 100050 (China)

[d] Prof. Y.-T. Zheng
Key Laboratory of Animal Models and Human Disease Mechanisms and Laboratory of Molecular Immunopharmacology
Kunming Institute of Zoology, Chinese Academy of Sciences
Kunming 650223, Yunnan (China)

Supporting information for this article is available on the WWW under http://dx.doi.org/10.1002/chem.200801092.

together with several known nortriterpenoids, including compounds **1**–**3** and lancifodilactone I (**5**),[8d] from the leaves and stems of *Schisandra rubriflora*. Herein, we report the isolation, structure elucidation, biological activity of compound **4**, and investigations of the biogenetic relationships among schisanartane nortriterpenoids (**1**, **4**, **5**) through transition-state investigations by using DFT at the B3LYP/6–311+G(d,p) level.

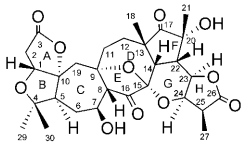

micrandilactone D (1)

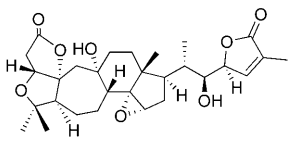

micrandilactone B (2)

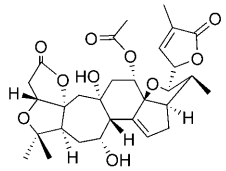

lancifodilactone A (3)

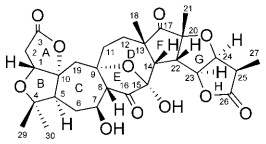

4

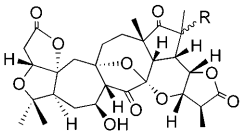

4a R = -OH
4b R = -OH

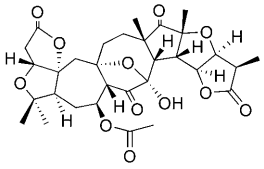

acetate derivative of 4

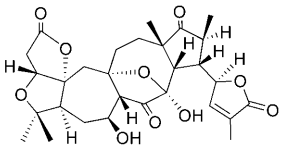

lancifodilactone I (5)

Results and Discussion

Rubriflordilactone C (**4**) was obtained as a colorless and optically active crystal, $[\alpha]_D^{23.7}=+27.79$ ($c=0.022$, MeOH). Its negative ESIMS displayed $[M-H]^-$ at m/z 599, corresponding to a molecular formula of $C_{29}H_{36}O_{11}$, as also determined by high-resolution electron-spray-ionization mass spectrometry (HRESIMS) ($[M-H]^-$, found 559.2181, calcd 559.2179). Thus, the structure of **4** possessed 12 degrees of unsaturation. The ^{1}H NMR spectrum (see Table S1 in the Supporting Information)[9] indicated three tertiary methyl groups and two secondary methyl groups. Analysis of the ^{1}H and ^{13}C NMR (see Table S1 in the Supporting Information)[9] and HSQC spectra revealed that **4** contained two ester groups, two carbonyl groups, five methyl groups, five methylene groups, nine methane groups (including four oxygenated ones), and six quaternary carbon atoms (including five oxygenated ones). Comparison of all these spectral data with those of the nortriterpenoids from the schisantane skeleton, which were previously reported from the *Schisandra* genus, suggested that compound **4** belongs to the same family and partially shares structural features with the known nortriterpenoid, micrandilactone D (**1**).[8a]

Analysis of 2D NMR data of **4**, including ^{1}H–^{1}H COSY, HSQC, and HMBC experiments, established the same planar substructure of rings A–F with those of compound **1** and the existence of a five-membered α-oxo-β-methyl-γ-lactone ring moiety attached to C22. According to the molecular formula, another ring should form in this structure. However, there is not enough spectroscopic evidence from 2D NMR studies to construct how the ring formed. Normally, there is an oxygen bridge between C15, C24, and ring G formed in the schisantane-skeleton nortriterpenoids as shown in **1**. For this reason, we originally considered that the last ring may also be formed by the same pattern. Accordingly, **4** was first deduced to have the same planar structure as **1**. However, the chemical shift of some carbon atoms in **4** differed considerably to those in **1**. Specifically, the chemical shifts of C20, C22, C23, and C24 were located at $\delta=74.7$, 41.6, 73.6, and 72.4 ppm in **1** and at $\delta=89.4$, 51.8, 87.4, and 84.4 ppm, respectively, in **4**. These differences may result from the changes of stereogenic centers as an unexpected ROESY correlation was observed in **4** between 14-H and 23-H. In addition, the obvious ROESY correlation and the small coupling constant between 23-H and 24-H suggest that 26-H and 24-H exist on the same face. The configuration of C(21)H_3 cannot be determined as not enough evidence was found from the ROESY spectrum. Thus, the structure was initially determined as either **4a** or **4b**.

The obvious structural difference between **4a** and **4b** with **1** is that both 23-H and 24-H were changed from α- to β-orientations. We are not sure if the configuration differences (at C23 and C24) can cause these large chemical shift differences. Thus, the structures still require solid evidence, such as X-ray analysis for unequivocal assignment. Unfortunately, we could not obtain crystals suitable for X-ray analysis. This barrier made us turn to computational methods.[10,11] In this way, we decided to calculate ^{13}C NMR shifts for the schisantane skeleton nortriterpenoids by using the gauge-independent atomic orbital (GIAO) method,[11] in which the B3LYP/6–311++G(2d,p)//B3LYP/6–31G(d) levels were employed to determine if this method could be applicable for the structure determination of **4**. Thus, micrandilactone D (**1**)

Abstract in Chinese:

从红花五味子(*Schisandra rubriflora*)中分离得到一个新奇的具有生物活性的降三萜红花五味子二内酯 (rubrifloradilactone) C (**4**)以及四个其他的降三萜化合物(**1-3, 5**)。红花五味子二内酯 C (**4**) 对 K562 和 HepG2 细胞系具有比顺铂(*cis*-platin)还强的细胞毒活性。并利用波谱数据分析、用 GIAO 理论方法在 B3LYP/6-311++G(2d,p)//B3LYP/6-31G(d)水平上计算的 ^{13}C NMR 数据比较以及 X－射线单晶衍射实验确定了化合物红花五味子二内酯 C 的结构。同时，利用 DFT 理论方法，在 B3LYP/6-311+G(d,p)的水平上，通过过渡态能量计算，从计算的角度阐明了小花五味子二内酯 D (**1**) 和红花五味子二内酯 C (**4**)关键的生源步骤。并根据该新的生源机制，对其他可能形成的产物进行了预测。

was selected for this test study first. The chemical shift predictions agreed well with the recorded shifts (see Table S2 in the Supporting Information).[9] Then, the proposed structures **4a** and **4b** were evaluated by the same method. Unfortunately, the computed ^{13}C NMR data for **4a** indicates chemical-shift differences of 9.9, 8.3, and 12.8 ppm versus the experimental results at C20, C22, and C23, respectively. Also, the calculated ^{13}C NMR data for **4b** had chemical-shift differences as high as 12.9, 8.4, and 18.6 ppm at C20, C21, and C23, respectively, compared with those observed. The big chemical-shift differences between the calculated shifts in **4a** or **4b** and experimental values suggested that **4a** and **4b** were not the correct structures.

To the best of our knowledge, if an isolated hydroxy group is attached at C24, it is impossible for the chemical shift of C24 to occur as far downfield as $\delta = 84.4$ ppm. That means there would be a new ring formed between ring H and ring F. The structure was thus deduced as **4**. The calculated ^{13}C NMR data agreed well with the experimental data (see Table S3 in the Supporting Information).[9] However, we did not find a related HMBC correlation between 24-H and C20 to support the calculated structure. However, after changing the solvent to [D_4]methanol, we found two important ROESY correlations of C(21)H_3 with C(27)H_3 and of 23-H with 25-H, which further supported the structure determined for **4**. Luckily, after the successful conversion of compound **4** to its acetate derivative at the 7-OH group, suitable crystals were obtained from its methanol solution after a long crystallization period. We also made sure that the acetate derivative of **4** did not change in the crystallization period by comparing the ^{1}H NMR spectra before and after crystallization. Thus, the X-ray diffraction crystal structure finally confirmed that the structure of **4** was correct (Figure 1). This result demonstrated that the current B3LYP/6–311++G(2d,p)//B3LYP/6–31G(d) computational methods could provide accurate computed ^{13}C NMR chemical shifts in the identification of complex natural products.

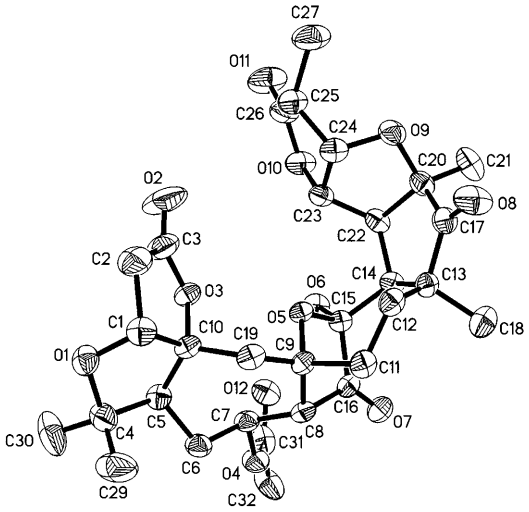

Figure 1. ORTEP plot of the X-ray structure of acetate of **4** depicting the relative stereochemistry.

Rubriflordilactone C (**4**) was evaluated for its cytotoxicity against two human tumor-cell lines, K562 and HepG2, by using the bioassay method previously described.[12] Compound **4** showed obvious inhibitory activities with IC_{50} values of 0.14 and 0.54 $\mu g\,mL^{-1}$ for K562 and HepG2, respectively (*cis*-platin: $IC_{50} = 0.40$ and 0.59 $\mu g\,mL^{-1}$, respectively). In addition, compound **4** was tested for cytotoxicity in an assay against C8166 cells (CC_{50}), and its anti-HIV-1 activity was evaluated by an inhibition assay for the cytopathic effects of HIV-1_{IIIB} (EC_{50}) by using 3′-azido-3′-deoxythymidine (AZT) as a positive control ($EC_{50=}0.0034$ $\mu g\,mL^{-1}$ and $CC_{50} > 200$ $\mu g\,mL^{-1}$).[13] These assays showed modest anti-HIV-1 activity with an EC_{50} value of 5.18 $\mu g\,mL^{-1}$ and cytotoxicity against C8166 cells with CC_{50} of 77.54 $\mu g\,mL^{-1}$ and a selectivity index (CC_{50}/EC_{50}) value of 14.9.

The intriguing occurrence of these five compounds (**1**–**5**) in the same plant led us to continue to study the relationship among these structures, especially among **1**, **4**, and **5**. A possible biogenetic transformation mechanism was originally proposed.[8a,j] Herein, we now propose a new biogenetic route for the formation of **1** and **4** from **5**, and, for the first time, we predict the structure of some possible natural products based on this mechanism.

Compound **4** is the first case of a schisanartane nortriterpenoid possessing a new ring system that is significantly different from micrandilactone D (**1**). This difference is that ring G in **4** is connected directly to the ring F, whereas ring G in **1** is connected with both ring D and ring F. The mechanism for ring-G formation in **1** could be the same as the mechanism we previously proposed; namely, the hydroxy group on C15 attacks the carbon C24 of the double bond (C=C).[8a] However, there is another important possibility. There should be an OH group on C24 in **5**. This OH group could react with OH groups on either C15 or C20 to form the corresponding natural products **1** and **4**, respectively.

Some key steps selected from the previously proposed biosynthetic route from schiartane skeleton to schisanartane are illustrated in Scheme 1.[8a] Two intermediates with different stereogenic centers on C25 would be formed when the OH group on C15 attacks the C=C (from **7** to **8**) based on the general chemical reaction mechanism. However, the *cis* isomer, **8**, shown in Scheme 1, which has the same structure as the natural product, should be the minor product according to this mechanism. The major product formed though this mechanism should be the *trans* isomer (**8a**). Isomer **8a** was not shown in the original route as the major structure. The mechanism of direct enolization of α,β-unsaturated lactones to the products was considered. However, for the same reason as discussed above, the major products formed should be the *trans* isomer instead of the *cis* isomer. In fact, during our research, we were never able to detect the *trans* isomer, which was predicted by the proposed mechanism[8a] and by the direct enolization mechanism.

Indeed, the hydroalkoxylation of unfunctionalized olefins is difficult and traditionally must be mediated by stoichiometric amounts of metal ions.[14] Catalytic processes for such

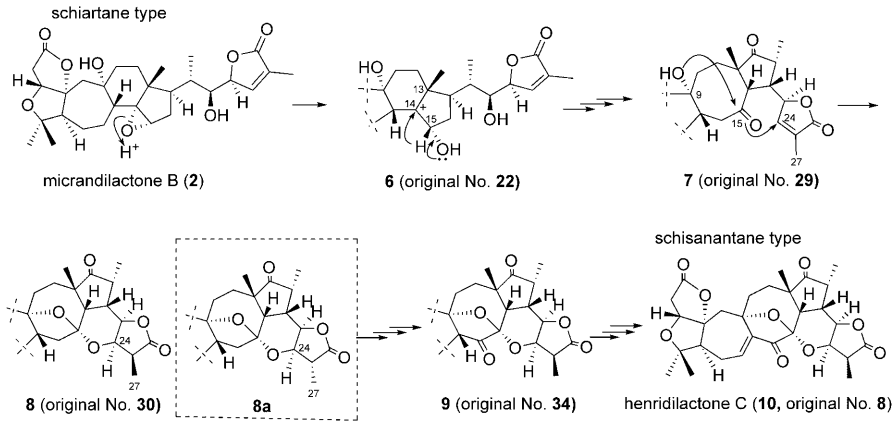

Scheme 1. Selected biosynthetic route (previously reported in reference [8a]).

transformations are necessary, however, they are limited.[15] To date, only silver,[16] platinum,[17] gold,[18] tin,[19] ruthenium,[20] and iridium[21] ions have been found as catalysts for intramolecular and intermolecular hydroalkoxylation of unfunctionalized olefins. In the intermolecular hydroalkoxylation of the functionalized olefins, catalysis by palladium ions is still required.[22] Similar intramolecular hydroalkoxylations of functionalized olefins was not found.

To determine if the reaction from **7** to **8** in Scheme 1 is reasonable, the transition state (TS) for the addition of OH groups to C=C was calculated at the B3LYP/6–311+G(d,p) level[23] by using the models shown in Scheme 2. The possible TSs without acidic catalysis are discussed first. Later, acid catalysis is considered as it could prevail within an enzyme.

Two ROH addition procedures were examined (routes 1 and 2). Route 1 involves direct OH attack on the C=C double bond. Route 2 considered the effect of water on the TS barriers. In this route, one OH group proton transfer to a H_2O is followed by a proton transfer from H_2O to C=C. These two routes contain six TS geometries. The lower calculated TS free-energy barrier through route 1 is 55.4 kcal mol^{-1} at the B3LYP/6–311+G(d,p) level (via **TS-2**) in the gas phase. This barrier is far too high for the addition to proceed. The lowest calculated TS barrier in route 2 is 51.5 kcal mol^{-1}. This barrier is also too high for the addition to take place.

Enzymatic catalysis may occur, which decreases the TS barrier. However, the exact enzyme is still unknown. Thus, a general method to use a solvent, which has a dielectric constant (ε) close to that of the interior of enzyme ($\varepsilon = 4.0$)[24] should be selected in the TS-barrier corrections. In this study, a neutral solvent, chloroform ($\varepsilon = 4.9$), was selected for the TS-barrier computations. These barrier computations were performed at both the B3LYP/6–311+G(d,p) and MP2/6–311+G(d,p) levels, respectively, by using the polarized continuum model (PCM)[25]. The barrier sequences follow the same order as that found in the gas phase. The activation energy to surmount **TS-2** is still predicted to be lower than that of **TS-1**.The lowest barrier among **TS-3** through **TS-6** is **TS-5**. In chloroform, the barrier through **TS-2** increased to 58.3 from 55.4 kcal mol^{-1} at the B3LYP/6–311+G-(d,p) level, and this barrier was 77.6 kcal mol^{-1} when computed at the MP2/6–311+G(d,p) level. The activation energy through **TS-5** decreased from 51.5 to 43.4 kcal mol^{-1} by using B3LYP/6–311+G(d,p) or increased to 67.3 kcal mol^{-1} at the MP2/6–311+G(d,p) level. These barrier values through **TS-2** and **TS-5** are so high that it is unreasonable for this hydroalkoxylation to take place.

The *cis*-isomer generation (through **TS-4** or **TS-6**) would encounter barriers of 85.9 and 86.1 kcal mol^{-1} at the B3LYP/6–311+G(d,p) level in the gas phase, respectively. These computed activation energies in chloroform were 69.2 kcal mol^{-1} or 71.7 kcal mol^{-1}, respectively, at the B3LYP/6–311+G(d,p) level. Furthermore, at the MP2/6–311+G(d,p) level, the barriers to **TS-4** and **TS-6** increased to 96.0 and 93.2 kcal mol^{-1}, respectively. No matter which method was employed, the calculated barriers are much too high for the addition of OH groups to occur across the double bond directly through routes 1 and 2.

The direct addition of water to C=C was also investigated at the B3LYP/6–311+G(d,p) level. There are six TS geometries found for the *trans*-addition route and six for *cis* addition. The lowest energy *trans*-addition pathway among the six possibilities passed though **TS-7** with a barrier of 57.6 kcal mol^{-1} in the gas phase. The lowest energy *cis*-addition barrier (**TS-8**) found was 90.2 kcal mol^{-1} among the six TS geometries. These **TS-7** and **TS-8** barriers decreased to 44.9 and 71.5 kcal mol^{-1} by using the PCM with chloroform as the solvent at the B3LYP/6–311+(d,p) level, respectively. These energy magnitudes, when corrected by the PCM, increased to 70.2 and 91.9 kcal mol^{-1}, respectively, at the MP2/6–311+G(d,p) level. Thus, conventional reactions under neutral conditions to form these natural products clearly seems to be impossible. The TS structures (**TS-1** to **TS-8**) are illustrated in Scheme 2.

Without acidic catalysis, we concluded that the major product formed would be the *trans* isomer instead of the *cis* isomer, which was required to form the known natural product. However, we cannot exclude the possibility that an acid-catalyzed enzymatic mechanism may exist to promote the addition reaction. Acidic catalysis might change the order of the transition state barriers in the pathways proceeding through **TS-3** through **TS-6**. Thus, the acidic catalytic routes through **TS-1H** to **TS-8H** were investigated at the B3LYP/6–311+G(d,p) level. The carbonyl group was first protonated at the oxygen moleculs, activating the carbonyl carbon through a positive charge increase on C24, which lowers the barrier for nucleophilic attack of the OH group

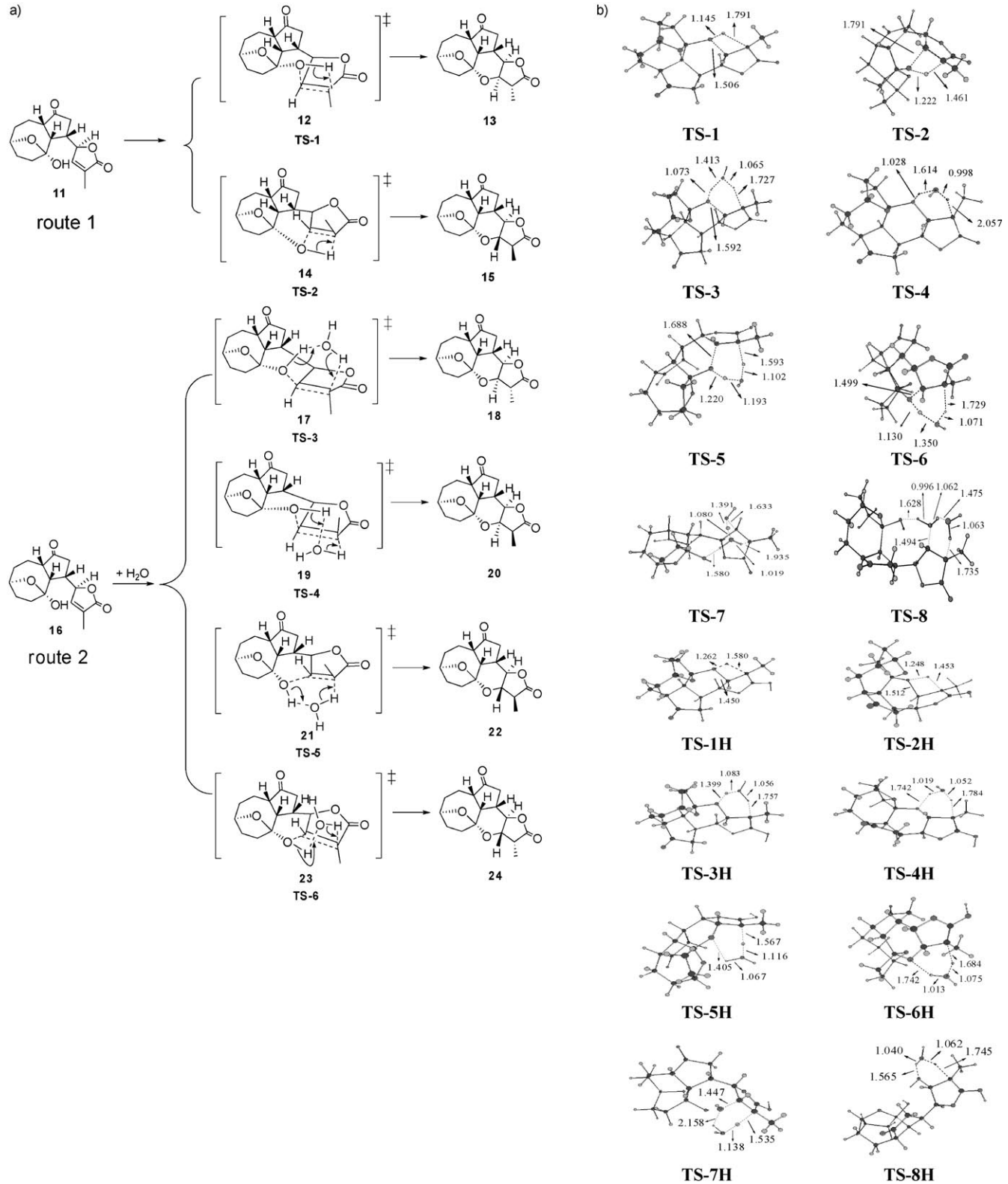

Scheme 2. a) The proposed model of the addition mechanism's transition states derived at the B3LYP/6–311+G(d,p) level. b) Ball-and-stick models of the above-derived transition states. The unit for bond lengths was Ångstroms.

on C24. The calculated barriers to **TS-1H** through **TS-8H** are illustrated in Table 1. Acidic catalysis decreased the TS barriers in all cases. The lower-energy pathway on comparing routes through **TS-1H** and **TS-2H** was through **TS-2H** with a barrier of 42.5 kcal mol^{-1} at the B3LYP/6–311+G(d,p) level in the gas phase. This barrier increased to 46.1 or

Table 1. TS barriers at the B3LYP/6–311+G(d, p) level in the gas phase and in chloroform (with energy in kcal mol^{-1}).

TS	$\Delta G1$[a]	$\Delta G2$[b]	$\Delta G3$[c]
TS-1[d]	77.8	76.9	94.1
TS-2	55.4	58.3	77.6
TS-3	61.1	49.4	73.1
TS-4	85.9	69.2	96.0
TS-5	51.5	43.4	67.3
TS-6	86.1	71.7	93.2
TS-7	57.6	44.9	72.0
TS-8	90.2	71.5	91.9
TS-1H[e]	64.7	68.1	86.7
TS-2H	42.5	46.1	61.0
TS-3H	37.4	28.1	43.8
TS-4H	57.5	45.9	61.0
TS-5H	25.2	17.9	34.3
TS-6H	58.3	46.9	62.3
TS-7H	36.9	24.3	39.9
TS-8H	60.6	50.1	68.4

[a] Barriers at the B3LYP/6–311+G(d,p) level, (single-point energy in the gas phase). [b] Barriers at the B3LYP/6–311+G(d,p) level (single-point energy in chloroform). [c] Barriers at the MP2/6–311+G(d, p) level (single-point energy in chloroform). [d] TS-*x* means transition-state structure number, $x=1$ to 8. [e] TS-*x*H refers to the number of the transition state's structure in which these transition states were each catalyzed by an acidic proton, $x=1$ to 8.

61.0 kcal mol^{-1} at the B3LYP/6–311+G(d,p) or MP2/6–311+G(d,p) levels, respectively, by using the PCM in chloroform. Thus, this path is unreasonable.

The lowest-energy pathway among the four routes through **TS-3H**, **TS-4H**, **TS-5H**, and **TS-6H** occurred through **TS-5H**. This barrier was 17.9 kcal mol^{-1} in chloroform at the B3LYP/6–311+G(d,p) level and increased to 34.3 kcal mol^{-1} at the MP2/6–311+G(d,p) level in chloroform. This produces the *trans* isomer. The direct *trans* addition of water to C=C, through **TS-7H**, had the lowest energy (24.3 kcal mol^{-1}) in chloroform at the B3LYP/6–311+G(d,p) level, or 39.9 kcal mol^{-1} at the MP2/6–311+G(d,p) level. This produced the *trans* isomer. The *cis*-addition barrier in chloroform (**TS-8H**) was much larger with a value of 50.1 kcal mol^{-1} at the B3LYP/6–311+G(d,p) level in chloroform or 68.4 kcal mol^{-1} at the MP2/6–311+G(d,p) level. The *cis*-isomer generation (through **TS-4H**, **TS-6H**, or **TS-8H)** also encountered higher energy barriers than the corresponding predicted activation energies to form the *trans* isomer, respectively.

Clearly, whether or not acid catalysis occurs, these addition reactions are difficult. Addition might be possible through **TS-5H** (17.9 kcal mol^{-1} at the B3LYP/6–311+G(d,p) level), but this would produce the *trans* isomer instead of the *cis* isomer. Of course, the *trans* isomer did not form in *S. rubriflora*. These calculated barriers explain why the OH group attack on C=C is so difficult and why the *cis* isomers can not be formed in this way. Obviously, the previously proposed biosynthetic route has drawbacks (Scheme 1).

The assistance of a special enzyme is needed to catalyze the formation of the obtained *cis* natural product. Thus, a key question emerged. Does the enzyme catalyze the formation of the natural products directly or is an intermediate, such as the *cis* isomer (OH and Me groups located at the same side on ring H), catalytically generated, which then proceed to the product? We favor the initial formation of the *cis* isomer. In this route, three factors must be considered carefully (Scheme 3). First, evidence is required to support formation of the hydroxy group on C24, located either *cis* or *trans* to the methyl group ($C(27)H_3$) located on C25. Secondly, the relative stereochemistry at C15, C20, and C24 should be maintained during the loss of water. Thus, the configurations at C15, C20, and C24 would remain unchanged. Finally, the two *cis* isomers would form products **1** and **4** after the loss of water, respectively.

Five-membered rings that are similar to ring H (α-oxo-β-methyl-γ-lactone ring) of schisanartane nortriterpernoids have been reported as both *cis* and *trans* isomers at the α and β positions in some natural products.[26] This means that the formation of a OH group on C24 is possibly catalyzed by special enzymes in vivo and the OH group could be formed in the *cis* position on C24. Further investigations have demonstrated that the configuration did not change during the intramolecular dehydration that occurs between the two ring hydroxy groups, even when the chemical reactions are carried out under very harsh conditions.[27] It is noteworthy that the configuration of C23 in the biogenetic precursor can either be *R* or *S* because both configurations are commonly found in five-membered α,β-unsatuated-γ-lactone rings in nature.[28] These conclusions are very significant for our new biogenetic pathway. The remaining question is whether or not **1** and **4** can be formed through this route as there are two possible intramolecular dehydration products formed between the two OH groups of each hydrated intermediate (**26**, **28**, **30**, **33**, **36**, **39**; Scheme 3).

As shown in Scheme 3, optimization of all the pairs of possible products were performed at the B3LYP/6–31G(d) and B3LYP/6–311+G(d,p) level in the gas phase, respectively. Frequency or eigenvalue analyses were carried out. Free energy, zero-point energy correction magnitudes, and total electronic energies were used in the relative energy comparisons by using the B3LYP/6–31G(d) method. Only total electronic energy was used by the B3LYP/6–311+G(d,p) method. As a result, the energy sequence between each pair of possible products was the same with the two methods. Especially notable, the energy differences are almost the same with the energetics after zero-point energy corrections at the B3LYP/6–31G(d) level as those obtained at the B3LYP/6–311+G(d,p) level. Therefore, it is possible to use the zero-point energy correction data at the B3LYP/6–31G(d) level to predict the major products formed in other similar procedures.

The formation of micrandilactone D (**1**) proceeds at lower energy, so kinetically, **1** would be the major product. Product **27**, lies 10.3 kcal mol^{-1} or 11.7 kcal mol^{-1} higher in energy than **1**. Thus, **27** could not be formed on this path. Indeed, product **27** was never found during our research. Thus, path 1 would form micrandilactone D (**1**) ($\approx$100%).

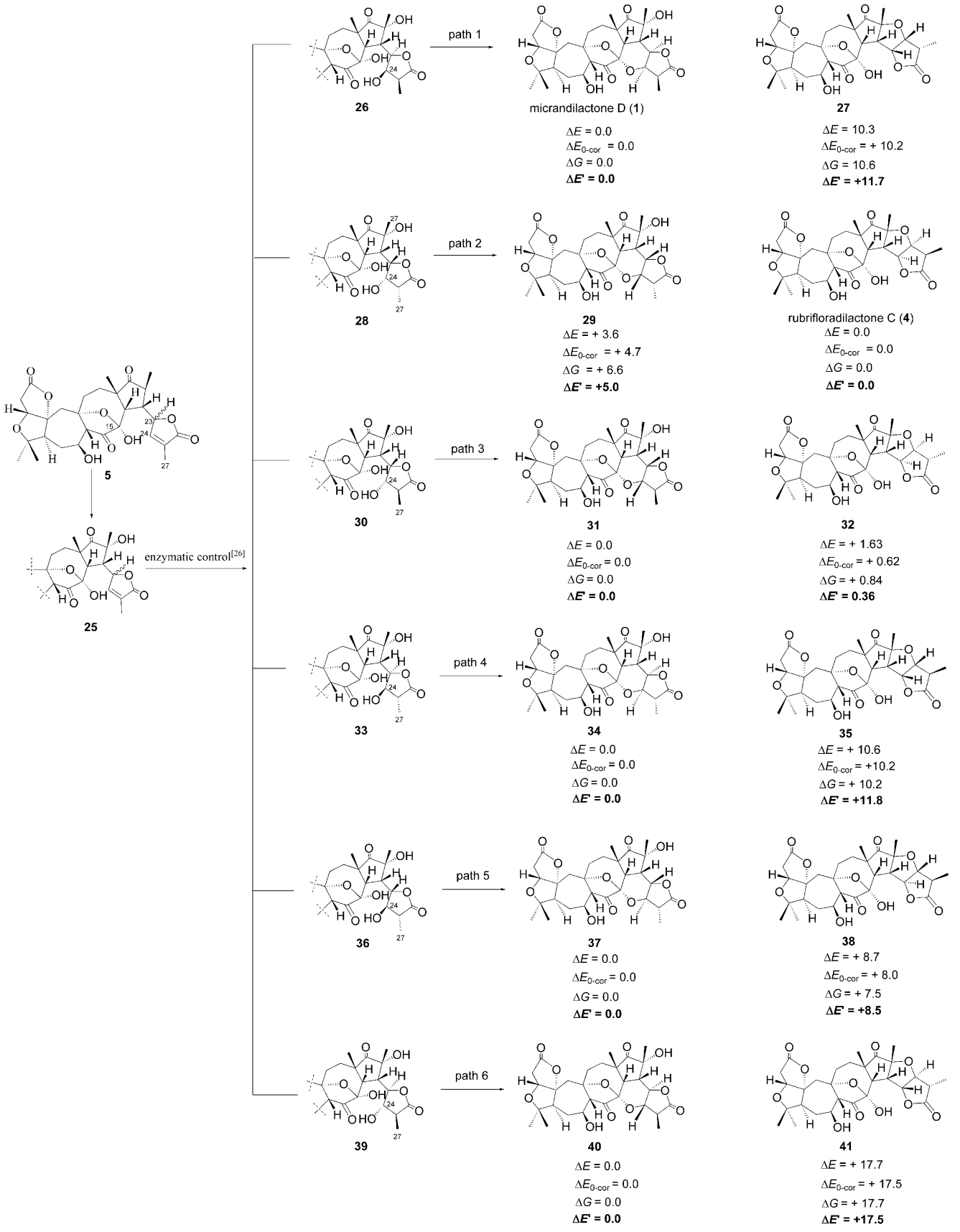

Scheme 3. Relative energies [kcal mol^{-1}] between each pair of compounds formed in the proposed biogenetic way. (ΔE = total electronic energy, $\Delta E_{0\text{-cor}}$ = energy after the zero-point energy correlation, ΔG = free energy). These data were obtained at the B3LYP/6–31G(d) level. The magnitudes of $\Delta E'$ that are shown in bold were obtained at the B3LYP/6–311+G(d,p) level.

If this route is general, then path 2 would lead to the formation of rubriflordilactone C (**4**). This conclusion was further strengthened by comparing the computed relative energies of the two products **4** and **29**. The expected compound rubriflordilactone C (**4**) is 3.6–6.6 kcal mol^{-1} lower in energy than product **29**. Thus, 97% of **4** would be found in nature if equilibrium was achieved based on the total computed electronic energy difference of 3.6 kcal mol^{-1}. This content increases to 99.8% when a free-energy difference of 6.6 kcal mol^{-1} was used. Only **4** could be found in our research.

In addition, *trans* isomers might be expected to exist in the plant as mentioned above. Thus, we predicted different products from the four possible *trans*-isomer intermediates (**30**, **33**, **36**, **39**) that could be formed by enzymatic catalysis. Each of these were evaluated at the B3LYP/6–31G(d) and B3LYP/6–311+G(d,p) levels (paths 3–6 in Scheme 3; the relative energy values are summarized below their structures). The products expected to be formed are both **31** (about 60–70%) and **32** (about 30–40%) through path 3, **34** (≈100%) through path 4, **37** (≈100%) through path 5, and **40** (≈100%) through path 6 by using the free-energy differences calculated and total electronic energy at the B3LYP/6–311+G(d,p) level and assuming equilibrium control. In addition, **40** might form through **TS-5H** as the **TS-5H** barrier was 17.9 kcal mol^{-1} at the B3LYP/6–311+G(d,p) level (Table 1). However, this barrier increased to 34.3 kcal mol^{-1} at the MP2/6–311+G(d,p) level. Thus, formation of **40** by this way could not be favorable.

Conclusion

In summary, determination of the biosynthetic pathway for schisanartane triterpenoid formation is a great challenge owing to their complex structures. Our present computational studies on the mechanism of ring-G formation in **1** and **4** led to the establishment of a part of this biogenetic route and improved our understanding of this series of nortriterpenoids from a biogenetic aspect. The predicted natural products based on this new biogenetic route still need to be experimentally validated. The proposed biosynthetic route remains a hypothesis until it has been confirmed by isotopic labeling and enzymatic studies. The computational methods, B3LYP/6–311++G(2d,p)//B3LYP/6–31G(d), can provide corrected predictions for ^{13}C NMR spectroscopy in complex natural-product identifications. Further investigation of the triterpenoid constituents from this genus and their biogenetic pathways is still in progress.

Experimental Section

General: Optical rotations were measured with a Horiba SEPA-300 polarimeter. UV spectra were obtained by using a Shimadzu UV-2401 A spectrophotometer. A Tenor 27 spectrophotometer was used for scanning IR spectroscopy with KBr pellets. 1D and 2D NMR spectra were recorded on Bruker AM-400 and DRX-500 spectrometers. Unless otherwise specified, chemical shifts (δ) were expressed in ppm with reference to the solvent signals. Mass spectra were performed on a VG Autospec-3000 spectrometer under 70 eV. Column chromatography was performed with silica gel (200–300 mesh, Qing-dao Marine Chemical, Inc., Qingdao, China). Preparative HPLC was performed on an Agilent 1100 liquid chromatograph with a Zorbax SB-C_{18}, 9.4 mm × 25 cm, column. Fractions were monitored by TLC and spots were visualized by heating silica gel plates sprayed with 10% H_2SO_4 in EtOH.

Plant material: The leaves and stems of *S. rubriflora* were collected in August 2003 from Dali Prefecture of Yunnan Province, China. The specimen was identified by Prof. Xi-Wen Li. A voucher specimen, No. KIB 2003–08–02, has been deposited at the State Key Laboratory of Phytochemistry and Plant Resources in West China, Kunming Institute of Botany, Chinese Academy of Sciences.

Extraction and isolation: Air-dried and powdered stems and leaves (3.1 kg) were extracted with 70% aqueous Me_2CO (4×5 L) at room temperature and concentrated in vacuo to give a crude extract (110 g), which was partitioned between H_2O and EtOAc. The EtOAc part (77.0 g) was chromatographed on a silica gel column eluting with $CHCl_3$/CH_3OH (1:0, 9:1, 8:2, 2:1, and 0:1) to afford fractions I–V. Fraction II (10.4 g) was repeatedly chromatographed on silica gel and Sephadex LH-20, and then by preparative HPLC (CH_3OH/H_2O, 42:58 and 45:55, and CH_3OH/CH_3CN/H_2O, 20:15:65 and 25:15:60) to yield **1** (10.2 mg), **2** (15.4 mg), **3** (20.1 mg), **4** (12.8 mg), and **5** (17.9 mg).

Rubrifloradilactone C (4): White powder; $[\alpha]_D^{23.7}=+27.79$ ($c=0.002$, MeOH); ^{1}H and ^{13}C NMR spectroscopy (see Table S1 in the Supporting Information);[9] IR (KBr): $\tilde{\nu}_{max}=3447$, 2975, 2934, 1762, 1636, 1457, 1378, 1171, 1104, 986 cm^{-1}; UV/Vis (MeOH): λ_{max} (log ε)=203 (3.14), 313 (2.25) nm; negative ESI-MS: m/z: 599 $[M-H]^-$; HRESIMS: m/z calcd for $C_{29}H_{35}O_{11}$ $[M-H]^-$: 559.2179; found: 559.2181.

Acetylaction of rubrifloradilactone C (4): The acetylaction procedure is to add the Ac_2O and pyridine to the substrate (**4**) at 0°C and this reaction was kept at room temperature for 12 h and afford the acetate product with almost 100% yield.

X-ray data for acetate derivative of rubrifloradilactone C (4): $C_{31}H_{38}O_{12}$, $M_r=606.61$, orthorhombic, space group $P2_12_12_1$, $a=12.760(3)$, $b=14.510(3)$, $c=16.907(3)$ Å, $V=3130.3(11)$ Å^3, $Z=4$, $\rho_{calcd}=1.297$ g cm^{-3}, crystal dimensions $0.43\times0.23\times0.10$ mm^3 was used for measurements on a MAC DIP-2030 K diffractometer with a graphite monochromator (ω-2θ scans, $2\theta_{max}=50.0°$), $Mo_{K\alpha}$ radiation. The total number of independent reflections measured was 6242, of which 3286 were observed ($|F|^2\geq2\sigma|F|^2$). Final indices: $R_{1\_}=0.058$, $WR_{2\_}=0.1462$, $S=1.035$. The crystal structure (acetate derivative of **4**) was solved by direct methods using SHELX-86[29] and expanded by using Fourier difference techniques, refined by the program and method NOMCSDP,[30] and the full-matrix least-squares calculations. CCDC-644472 contains the supplementary crystallographic data for this paper. These data can be obtained free of charge from The Cambridge Crystallographic Data Centre via www.ccdc.cam.ac.uk/data_request/cif.

Computational methods: The computations of TS barriers involved in the research were performed at B3LYP/6–311+G(d,p) level. Frequency was also calculated at the same level and one imaginary frequency was found for each TS structure. Since the dielectric constant (ε) in the interior of enzyme was about 4.0,[24] and the real enzyme in our research is unknown, an approximate method was used to estimate the catalytic effect. Chloroform, which has a dielectric constant value of 4.9 was used in the calculation for all geometries involved in the study. The PCM was selected for the calculation at the B3LYP/6–311+G(d,p) and MP2/6–311+G(d,p) levels. The optimization of all six pairs of possible products were performed at the at the B3LYP/6–31G(d) and B3LYP/6–311+G(d,p) levels, respectively.

Acknowledgements

We thank the reviewers for their valuable advice. This work was supported by grants from Xibuzhiguang Project from CAS to W.-L. Xiao and Cooperation Fund of CAS (YZ-06–01), the National Natural Science Foundation of China (30770235), the Yong Academic and Technical Leader Raising Foundation of Yunnan Province (2006PY01–47), Key Scientific and Technological projects of China and Yunnan Province (2004A719A14, 2004NG12, and 2005B0048M), the Natural Science Foundation of Yunnan Province (2005XY04 and 2006B0042Q), and the Mississippi State University Education and General budget provided support to C.U.P.

[1] R. Xu, G. C. Fazio, S. P. T. Matsuda, *Phytochemistry* **2004**, *65*, 261–291.
[2] P. Dzubak, M. Hajduch, D. Vydra, A. Hustova, M. Kvasnica, D. Biedermann, L. Markova, M. Urban, J. Sarek, *Nat. Prod. Rep.* **2006**, *23*, 394–411.
[3] D. R. Phillips, J. M. Rasbery, B. Bartel, S. P. T. Matsuda, *Current Opinion in Plant Biology* **2006**, *9*, 305–314.
[4] S. B. Mahato, S. Sen, *Phytochemistry* **1997**, *44*, 1185–1236.
[5] S. B. Mahato, A. K. Nandy, G. Roy, *Phytochemistry* **1992**, *31*, 2199–2249.
[6] a) M. Nishizawa, A. Yadav, Y. Iwamoto, H. Imagawa, *Tetrahedron* **2004**, *60*, 9223–9234; b) D. Q. Gao, Y. K. Pan, *J. Am. Chem. Soc.* **1998**, *120*, 4045–4046.
[7] a) J. B. Chang, J. Reiner, J. X. Xie, *Chem. Rev.* **2005**, *105*, 4581–4609; b) L. Opletal, H. Sovová, M. Bártlová, *J. Chromatogr. B.* **2004**, *812*, 357–371.
[8] a) R. T. Li, W. L. Xiao, Y. H. Shen, Q. S. Zhao, H. D. Sun, *Chem. Eur. J.* **2005**, *11*, 2989–2996; b) R. T. Li, Q. B. Han, Y. T. Zheng, R. R. Wang, L. M. Yang, Y. Lu, S. Q. Sang, Q. T. Zheng, Q. S. Zhao, H. D. Sun, *Chem. Commun.* **2005**, 2936–2938; c) R. T. Li, S. H. Li, Q. S. Zhao, Z. W. Lin, H. D. Sun, Y. Lu, C. Wang, Q. T. Zheng, *Tetrahedron Lett.* **2003**, *44*, 3531–3534; d) W. L. Xiao, H. X. Huang, L. Zhang, R. R. Tian, L. Wu, X. L. Li, J. X. Pu, Y. T. Zheng, Y. Lu, R. T. Li, Q. T. Zheng, H. D. Sun, *J. Nat. Prod.* **2006**, *69*, 650–653; e) W. L. Xiao, R. T. Li, S. H. Li, X. L. Li, H. D. Sun, Y. T. Zheng, R. R. Wang, Y. Lu, C. Wang, Q. T. Zheng, *Org. Lett.* **2005**, *7*, 1263–1266; f) W. L. Xiao, J. X. Pu, Y. Chang, X. L. Li, H. X. Huang, L. M. Yang, L. M. Li, Y. Lu, Y. T. Zheng, R. T. Li, Q. T. Zheng, H. D. Sun, *Org. Lett.* **2006**, *8*, 1475–1478; g) W. L. Xiao, L. M. Yang, N. B. Gong, L. Wu, R. R. Wang, J. X. Pu, X. L. Li, S. X. Huang, Y. T. Zheng, R. T. Li, Y. Lu, Q. T. Zheng, H. D. Sun, *Org. Lett.* **2006**, *8*, 991–994; h) R. T. Li, W. Xiang, S. H. Li, Z. W. Lin, H. D. Sun, *J. Nat. Prod.* **2004**, *67*, 94–97; i) R. T. Li, Y. H. Shen, W. Xiang, H. D. Sun, *Eur. J. Org. Chem.* **2004**, 807–811; j) X. H. Sheng, R. T. Li, J. P. Liu, Y. Lu, Y. Chang, C. Lei, W. L. Xiao, L. B. Yang, Q. T. Zheng, H. D. Sun, *Org. Lett.* **2007**, *9*, 2079–2082; k) R. T. Li, Q. S. Zhao, S. H. Li, Q. B. Han, H. D. Sun, Y. Lu, L. L. Zhang, Q. T. Zheng, *Org. Lett.* **2003**, *5*, 1023–1026; l) S. X. Huang, L. B. Yang, W. L. Xiao, C. Lei, J. P. Liu, Y. Lu, Z. Y. Weng, L. M. Li, R. T. Li, J. L. Liu, Q. T. Zheng, H. D. Sun, *Chem. Eur. J.* **2007**, *13*, 4816–4822; m) W. L. Xiao, X. L. Li, R. R. Wang, L. M. Yang, L. M. Li, S. X. Huang, J. X. Pu, Y. T. Zheng, R. T. Li, H. D. Sun, *J. Nat. Prod.* **2007**, *70*, 1056–1059; n) C. Lei, S. X. Huang, J. J. Chen, J. X. Pu, L. M. Li, W. L. Xiao, J. P. Liu, L. B. Yang, H. D. Sun, *Helv. Chim. Acta* **2007**, *90*. 1399–1405; o) J. Ren, W. L. Xiao, H. D. Sun, H. J. Zhu, *Eighth Tetrahedron Symposium*, Berlin, Germany, **2007**, P1, 145.
[9] Tables S1–S3 are in the Supporting Information.
[10] M. J. Frisch, et al, *Gaussian 03 User's Reference* Gaussian Inc. **2003**, Carnegie, PA. 15106, USA; see Supporting Information.
[11] a) D. Z. Liu, F. Wang, T. G. Liao, J. G. Tang, W. Steglich, H. J. Zhu, J. K. Liu, *Org. Lett.* **2006**, *8*, 5749–5752; b) K. Wolinski, J. F. Hilton, P. Pulay, *J. Am. Chem. Soc.* **1990**, *112*, 8251–8260.
[12] A. Monks, D. Scudiero, P. Skehan, R. Shoemaker, K. Paull, D. Vistica, C. Hose, J. Langley, P. Cronise, A. Vaigro-Wolff, *J. Natl. Cancer Inst.* **1991**, *83*, 757–766.
[13] J. H. Wang, S. C. Tam, H. Huang, D. Y. Ouyang, Y. Y. Wang, Y. T. Zheng, *Biochem. Biophys. Res. Commun.* **2004**, *317*, 965–971.
[14] R. C. Larock, W. W. Leong, *Comprehensive Organic Synthesis, Vol. 4*, Pergamon Press, New York, **1991**.
[15] M. Beller, J. Seayad, A. Tillack, H. J. Jiao, *Angew. Chem.* **2004**, *116*, 3448–3479; *Angew. Chem. Int. Ed.* **2004**, *43*, 3368–3398.
[16] C. G. Yang, N. W. Reich, Z. J. Shi, C. He, *Org. Lett.* **2005**, *7*, 4553–4556.
[17] H. Qian, X. Han, R. A. Widenhoefer, *J. Am. Chem. Soc.* **2004**, *126*, 9536–9537.
[18] C. G. Yang, C. He, *J. Am. Chem. Soc.* **2005**, *127*, 6966–6967.
[19] L. Coulombel, I. Favier, E. Duñach, *Chem. Commun.* **2005**, 2286–2288.
[20] Y. Oe, T. Ohta, Y. Ito, *Synlett* **2005**, 179–181.
[21] H. V. Grant, B. Liu, *Tetrahedron Lett.* **2005**, *46*, 1237–1239.
[22] T. Hosokawa, T. Shinohara, Y. Ooka, S. I. Murahashi, *Chem. Lett.* **1989**, 2001–2004.
[23] a) S. Y. Wan, H. Gunaydin, K. N. Houk, P. E. Floreancig, *J. Am. Chem. Soc.* **2007**, *129*, 7915–7923; b) P. S. Lee, W. Du, D. L. Boger, W. L. Jorgensen, *J. Org. Chem.* **2004**, *69*, 5448–5453; c) D. Marković, A. Varela-Álvarez, J. A. Sordo, P. Vogel, *J. Am. Chem. Soc.* **2006**, *128*, 7782–7795; d) J. Pfaendtner, X. R. Yu, L. J. Broadbelt, *J. Phys. Chem. A* **2006**, *110*, 10863–10871; e) N. J. Mosey, K. M. Baines, T. K. Woo, *J. Am. Chem. Soc.* **2002**, *124*, 13306–13321; f) Y. T. Di, H. P. He, Y. S. Wang, L. B. Li, Y. Lu, J. B. Gong, X. Fang, N. C. Kong, S. L. Li, H. J. Zhu, X. J. Hao, *Org. Lett.* **2007**, *9*, 1355–1358; g) L. C. Li, J. Ren, T. G. Liao, J. X. Jiang, H. J. Zhu, *Eur. J. Org. Chem.* **2007**, 1026–1030.
[24] R. R. Gabdoulline, R. C. Wade, *J. Mol. Biol.* **2001**, 1139–1155.
[25] a) S. Miertus, E. Scrocco, J. Tomasi, *Chem. Phys.* **1981**, *55*, 117–129; b) J. Tomasi, B. Mennucci, E. Cancès, *J. Mol. Struct.* **1999**, *464*, 211–226; c) M. Cossi, G. Scalmani, N. Rega, V. Barone, *J. Chem. Phys.* **2002**, *117*, 43–54.
[26] a) D. S. Ming, A. Lopez, B. J. Hillhouse, C. J. French, J. B. Hudson, G. H. N. Towers, *J. Nat. Prod.* **2002**, *65*, 1412–1416; b) B. N. Ravi, R. J. Wells, *Aust. J. Chem.* **1982**, *35*, 105–112; c) M. T. Pupo, P. C. Vieira, J. B. Fernandes, M. F. G. F. Silva, *Phytochemistry* **1998**, *48*, 307–310; d) N. P. Lopes, D. H. S. Silva, M. J. Kato, M. Y. Yoshida, *Phytochemistry* **1998**, *49*, 1405–1410; e) M. H. Chaves, N. F. Roque, *Phytochemistry* **1997**, *44*, 523–528; f) P. C. Vieira, M. Yoshida, O. R. Gottlieb, H. F. P. Filho, T. J. Nagem, R. B. Filho, *Phytochemistry* **1983**, *22*, 711–713; g) K. W. Cho, H. S. Lee, J. R. Rho, T. S. Kim, S. J. Mo, J. Shin, *J. Nat. Prod.* **2001**, *64*, 664–667; h) B. S. Min, S. Y. Lee, J. H. Kim, O. K. Kwon, B. Y. Park, R. B. An, J. K. Lee, H. I. Moon, T. J. Kim, Y. H. Kim, H. Joung, H. K. Lee, *J. Nat. Prod.* **2003**, *66*, 1388–1390; i) M. Lorenzo, I. Brito, M. Cueto, L. D′Croz, J. Darias, *Org. Lett.* **2006**, *8*, 5001–5004.
[27] a) I. C. Coste-Manière, J. P. Zahra, B. Waegell, *Tetrahedron Lett.* **1988**, *29*, 1017–1020; b) S. Wilmouth, H. Pellissier, M. Santelli, *Tetrahedron* **1998**, *54*, 10079–10088; c) S. Wilmouth, L. Toupet, H. Pellissier, M. Santelli, *Tetrahedron* **1998**, *54*, 13805–13812.
[28] a) R. Tanaka, H. Aoki, S. Wada, S. Matsunaga, *J. Nat. Prod.* **1999**, *62*, 198–200; b) R. Tanaka, S. Matsunaga, *J. Nat. Prod.* **1991**, *54*, 1337–1344; c) S. Hasegawa, N. Kaneko, Y. Hirose, *Phytochemistry* **1987**, *26*, 1095–1099; d) A. F. Barrero, J. F. Sanchez, E. J. Alvarez-Manzaneda, M. Munoz, A. Haidour, *Phytochemistry* **1992**, *31*, 615–620; e) R. Tanaka, H. Aoki, T. Mizota, S. Wada, S. Matsunaga, H. Tokuda, H. Nishino *Planta Med.* **2000**, *66*, 163–168; f) R. Tanaka, S. Matsunaga, *Phytochemistry* **1991**, *30*, 1983–1987; g) J. P. Kutney, D. S. Grierson, G. D. Knowles, N. D. Westcott, *Tetrahedron* **1973**, *29*, 13–20; h) F. H. Allen, J. P. Kutney, J. Trotter, N. D. Westcott, *Tetrahedron Lett.* **1971**, *3*, 283–286.
[29] G. M. Sheldrick, University of Gottingen, Gottingen, Germany, **1985**.
[30] Y. Lu, B. M. Wu, *Chin. Chem. Lett.* **1992**, *3*, 637–640.

Received: June 5, 2008
Published online: November 10, 2008

